Benchmarking bias: Expanding clinical AI model card to incorporate bias reporting of social and non-social factors

Carolina A. M. Heming, MD[1], Mohamed Abdalla, PhD[2], Monish Ahluwalia, MSc, MD[3], Linglin Zhang, MS[4], Hari Trivedi, MD[5], MinJae Woo, PhD[4], Benjamin Fine MD, MSc[2,6] Judy Wawira Gichoya, MD[5], Leo Anthony Celi, MD, MPH, MSc[7,8] , Laleh Seyyed-Kalantari, PhD[6,9]

1. Department of Radiology, Instituto Nacional do Câncer, Pr. da Cruz Vermelha, 23 - Centro, Rio de Janeiro, 20230-130, Brazil.
2. Institute for Better Health, Trillium Health Partners, 100 Queensway West, 6th floor, Mississauga, ON L5B 1B8, Canada
3. Kingston Health Sciences Centre, Queen’s University, 76 Stuart St., Kingston, ON K7L 2V7, Canada
4. School of Data Science and Analytics, Kennesaw State University, 3391 Town Point Dr NW, Kennesaw, GA 30144, USA
5. Department of Radiology and Imaging Sciences, Emory University, 1364 E Clifton Rd NE, Atlanta, GA 30322, USA
6. Vector Institute of Artificial Intelligence, 661 University Ave Suite 710, Toronto, ON M5G 1M1, Canada
7. Massachusetts Institute of Technology, 77 Massachusetts Avenue Cambridge, MA 02139, USA
8. Harvard Medical School , 25 Shattuck St, Boston, MA 02115, USA
9. Department of Electrical Engineering and Computer Science, York University, 4700 Keele St, Toronto, Ontario, ON M3J 1P3, Canada

Corresponding Author: Carolina A. M. Heming[1]

[1]Present Address: Iowa University Clinics and Hospital, 200 Hawkins Dr, Radiology Department, Office 3887, Iowa City, Iowa, IA 52240, USA

Abstract:

Clinical AI model reporting cards should be expanded to incorporate a broad bias reporting of both social and non-social factors. Non-social factors consider the role of other factors, such as disease dependent, anatomic, or instrument factors on AI model bias, which are essential to ensure safe deployment.

Keywords: Model fact cards, bias, fairness, artificial intelligence, medical imaging

1.Introduction:

Artificial intelligence (AI) models in healthcare often achieve performance on par with human specialists[1,2]. However, AI models with high performance on the overall population may have performance disparities for specific sub-populations. Discrepancies in AI model performance between sub-populations have been widely demonstrated in many applications. For example, race and sex bias has been reported in AI models developed for medical image disease diagnosis[3]. Patients' self-reported race can be detected from their medical images alone[4] by AI algorithms, and it is known that some algorithms may also have worse performance for historically underserved races (e.g. Hispanic or Black patients).

Such biases in healthcare AI-based decision-making tools are a critical issue that must be communicated, understood, and addressed before large-scale adoption. The model facts label was proposed to report clinical AI model performance to end users e.g., clinical staff[5]. However, the overall performance report does not demonstrate the full picture of how, when, and under what circumstances the model works or fails. Mitchell et al. introduce a model card for non-healthcare applications, which includes fairness analysis[6]. Considering the potential critical direct impact of healthcare AI model failures on human lives, including thorough bias analysis in the model card is crucial.

Moreover, AI models bias analysis often has focused only on investigating inequitable outcomes between different races and sexes[4,7,8]. Such a narrow focus misses other sources of bias and does not consider heterogeneity within members of a specific race/sex subgroup. For example, consider the case of a commercial algorithm that identified Black patients as having fewer healthcare needs than White patients with similar medical conditions. This occurred because the model used healthcare costs as a proxy to health status and Black patients often spent less on healthcare than White patients due to socioeconomic reasons[8]. If this model was debiased simply by correcting predictions for Black patients, the model would still harm low-income patients of all other races since income level cannot be universally attributed to race. Therefore, race is the incorrect bias factors to correct for in this instance.

2.Theory:

In this work, we suggest that:

2.1) model fact cards in health applications should be required to report thorough bias analysis outcomes to the end user,

2.2) bias analysis needs to highlight disparities with respect to *social* sensitive attributes in a broader regime beyond the well-known sex and race to capture the impact of other factors such as socioeconomic status, education, etc.

2.3) bias analyses need to be expanded to *non-social* factors that can be considered as sensitive attributes. The non-social factors may include (1) **anatomic factors** (e.g., body habitus, anatomic variants), (2) **disease-dependent factors** (e.g., disease appearance), (3) **instrumental factors** (e.g., imaging devices), and (4) **data sources**. Expanding bias reporting to *non-social* factors reveals other hidden disparity drivers, and allows clear and accurate communication of model biases and limitations to the end user and policy makers.

3. Methods:

We use two demonstrative model cards which report AI models outcome across different performance metrics for both social and non-social factors. Figure 1 shows the model card of an AI model trained on the CheXpert dataset, externally validated on a dataset of 200,000 chest x-rays from a tertiary care center[9]. Figure 2 demonstrates the model card for the imaging abnormality classification in screening mammogram analysis[10]. Model cards often include model details and information on what data the model has been trained on. In addition, for a given metric $M \in \{Accuracy, F1\ score, sensitivity, specificity, AUC, \ldots\}$, we have reported $\Delta M = M_{subgroup} - M_{overall}$, which demonstrates how much gap the subgroup measure of metric M, $M_{subgroup}$, is experiencing compared to the overall population, $M_{overall}$. A positive gap means the model performs in favor of the given subgroup, while the negative gap demonstrates the subgroup is unfavorable.

4.Results and Discussion:

<u>4.1 The impact of social factors on disparate AI outcomes</u>

Equality in model performance across subpopulations of a given sensitive attribute has been the focus of bias analysis[3,11,12]. The impact of social factors such as patient race and sex on disparate outcomes of AI models in health care has been widely demonstrated[4,7,8,13]. However, with much less attention to disparate outcomes of AI models with respect to other social factors such as patients' language (English vs. non-English speaker)[14], education[13], income level[13], age[3], or insurance type[3] have been demonstrated. For example, in a systematic study of AI-based chest X-ray prediction, Kalantari *et al.* found that AI models underdiagnosed historically under-served patients, e.g., such as younger patients or patients with Medicaid insurance type who are often low-income at a higher rate[3]. Also, Zhang *et al.* perpetuated undesired biases, resulting in performance discrepancies with respect to patients' spoken language (English vs. non-English), ethnicity, and insurance type[14]. Moreover, Pierson *et al* demonstrate bias with respect to the patients' education and income level in pain and disease severity measure[13]. Such studies demonstrate the importance of widely expanding the social sensitive attributes to include such factors as described. In Figure 1 and 2, you can see the disparate outcome of both AI models for chest X-ray and the mammography abnormality detection across sex, age and race. We prefer to report these quantities for all proposed social factors but we have been limited by the data availability for some factors.

<u>4.2 Non-social factors impact disparate AI model outcome</u>

In addition to social factors, there are non-social factors that can contribute to AI model bias which results in disparate outcomes and bias for groups of patients. These non-social factors may have a great impact on end-users' ability to trust the predictions of AI models in their specific practice. For example, if an AI model constantly has lower performance on patients whose image is gathered using a specific imaging device[9], then the end-user can be informed about this shortcoming in the model card and rely on the outcome of AI model accordingly. Here, we list some non-social factors that we suggest should be considered in the context of AI models for radiology applications.

4.2.1. Anatomic factors:

Anatomic variants and prior conditions may cause errors in diagnosis and treatment planning. For example, anatomic variants in the spine may be a source of inaccurate radiotherapy planning[15]. Similarly, anatomic variants can also be a source of inaccuracy in machine learning models for organ or tumor segmentation[16]. Oakden-Rayner *et al.* found that a classifier for hip fracture detection on frontal X-rays performed worst in cases with abnormal bone or joint appearance, such as Paget´s disease of the bone[17].

Additionally, differences in body habitus may affect model predictions. For instance, increased breast density is an independent risk factor for breast cancer[18] and simultaneously reduces mammography´s sensitivity in breast cancer screening[19]. Disparate AI model performance across breast density has been shown in Fig. 2 which is an illustrative example. Therefore, higher breast density in Asian and Black patients[20] may result in disparities for AI models due to breast density, not the race. In this example, adjusting model predictions based on race to reduce bias would be inappropriate for two reasons: (1) Asian or Black women with low breast density are now at higher risk of false positives, and (2) White women with high breast density will continue to be underdiagnosed. Rather than adjusting for race, predictions should be adjusted based on breast density.

4.2.2. Disease-dependent factors:

The same disease, but with different expressions, may also affect model performance. COVID-19 pneumonia may have different expressions according to the viral variant, immunization status and phase of the disease (early infection, pulmonary phase or hyperinflammatory phase)[21]. For instance, studies show that in hospitalized patients with COVID-19, CT was more likely to be negative for pneumonia during periods of Omicron versus Delta variant prevalence and that the proportion of patients with an atypical CT pattern was higher in the Omicron variant group than in the Delta variant group. Therefore, models developed to diagnose COVID-19 pneumonia should take into account those variables in order to not underdiagnose people with less severe disease[21]. In Figure 2 disparate outcomes of AI models across disease dependent factors including mass, architectural distortion, calcification and asymmetry has been demonstrated. Therefore, patients' disease labels have an impact on the model performance.

Another factor that influences different expressions for the same disease is the patient immunity, whether immunocompetent or immunocompromised. It is known that pulmonary tuberculosis also may present with different chest CT findings in HIV patients in comparison to immunocompetent patients[22]. Even different types of immunodeficiency may lead to variability in disease expression. For instance, the pulmonary manifestations of *Pneumocystis jirovecii* pneumonia might have different chest CT patterns between HIV-positive patients compared to patients with other reasons of immunosuppression, as in hematooncologic and posttransplant patients and in patients under immunosuppressive drugs due to autoimmune diseases[23]. Those differences, if not recognized, may be a source of disparity in the correct diagnosis of patients that require more complex care.

Variable tumor appearance may also impact model performance in specific subgroups. For example, pancreatic adenocarcinoma may be isoattenuating in up to 5.4% of cases making them visually indistinguishable from the surrounding pancreatic parenchyma on dynamic CT imaging and difficult to diagnose[24]. Therefore, the consistently lower sensitivity of an AI model for specific tumor appearance could result in disparate outcomes.

4.2.3. Instrumental factors:

AI model performance for face detection may vary depending on what cameras are used[6]. This is also the case in medical imaging: Ahluwalia et al. observed that the performance of AI models trained for abnormality classification varied substantially across different imaging devices in radiology[9,10]. For example, as shown in Figure 1, there is a 23% difference in sensitivity and specificity when applied to images taken using the GE Type 1 compared to images taken using a Varian Type 1. Similar disparate outcomes for AI model trained for mammography screening have been observed across imaging devices. (See model card in Figure 2, ΔAUC and ΔF1 score across imaging devices).

4.2.4. Data source:

Data sources (i.e., the type of hospital and patient population) impact model performance. For instance, as previously shown models trained on the CheXpert[25] dataset, which has more tertiary care centers cases, have less bias[3] than models trained on Chest-Xray14 which is gathered from a hospital that does not do routine procedures[3]. Additionally, model performance differs even across multiple departments within the same hospital. External validation of four AI models trained on four different datasets for the same disease classification task demonstrated reduced sensitivity, but increased specificity, in emergency room patients. The reverse was true for inpatients and ICU patients[9]. (See model card in Figure 1 for ΔM across different departments within the same hospital). Similarly for mammography screening AI models, we can find the disparate outcome of AI models across different departments in the hospital (See ΔM in Figure 2). The disparate outcomes across data sources must be evaluated and communicated to the end user to ensure appropriate, safe, and fair implementation of AI models into clinical care.

Model Facts Card – Chest Radiograph Classification

Model Details
- State-of-the-art convolutional neural network with a 121-layer DenseNet architecture developed by Kalantari et al., 2020 based on the CheXpert Image dataset
- Classifies chest radiographs into one or more of 14 classes: atelectasis, cardiomegaly, consolidation, edema, enlarged cardiomediastinum, fracture, lung lesion, lung opacity, pleural effusion, pleural other, pneumonia, pneumothorax, support devices, and no finding
- The no finding category was used to determine binary classes (normal if 1, abnormal if 0)

Intended Use:
- Chest radiograph classification for research purposes only

Factors:
- **Groups** include age, EHR-reported sex, and name-based ancestry (Greater European, Greater African/ Indian, and Greater East Asian), and 12 pathology classes
- **Instrumentation factors** include 8 chest radiograph imaging systems
- **Environment factors** include patient location (emergency room, inpatient, outpatient, and ICU)
- Other **relevant factors** not studied include image quality and rotation

Metrics:
- **Evaluation metrics** include accuracy, positive predictive value (PPV), negative predictive value (NPV), sensitivity, and specificity for each factor and group; sensitivity is provided for pathology classes
- Metrics were calculated from respective confusion matrices
- Bootstrap resampling (n = 10,000) was used to generate 95% confidence intervals

Training & Evaluation Data:
- **Trained** on 224,316 chest radiographs from Stanford University Medical Center between October 2002 and July 2017 (Irvin et al., 2019); no retraining nor threshold adjustment was performed
- **Evaluated** on 197,540 chest radiographs from Trillium Health Partners from January 2016 to December 2020 (Ahluwalia et al., 2023)

Caveats & Recommendations:
- Only applicable to Trillium Health Partners

Quantitative Analysis:
- Accuracy of 76% in binary classification with skewing to higher specificity vs. sensitivity
- Higher sensitivity in detecting pleural effusions; lower sensitivity in detecting cardiomegaly, fracture, and all pathologies when solitary
- Low sensitivity and high specificity in patients under 40 and in the emergency room
- High sensitivity and low specificity in patients over 65 and in the ICU
- Similar performance relative to sex and ancestry; variable performance on different equipment models

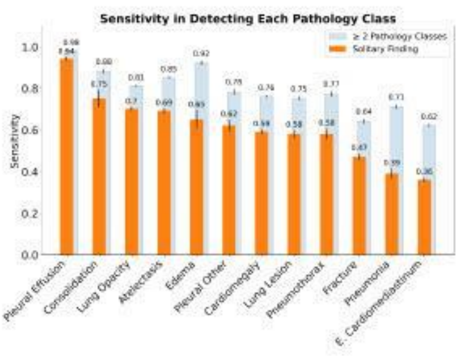

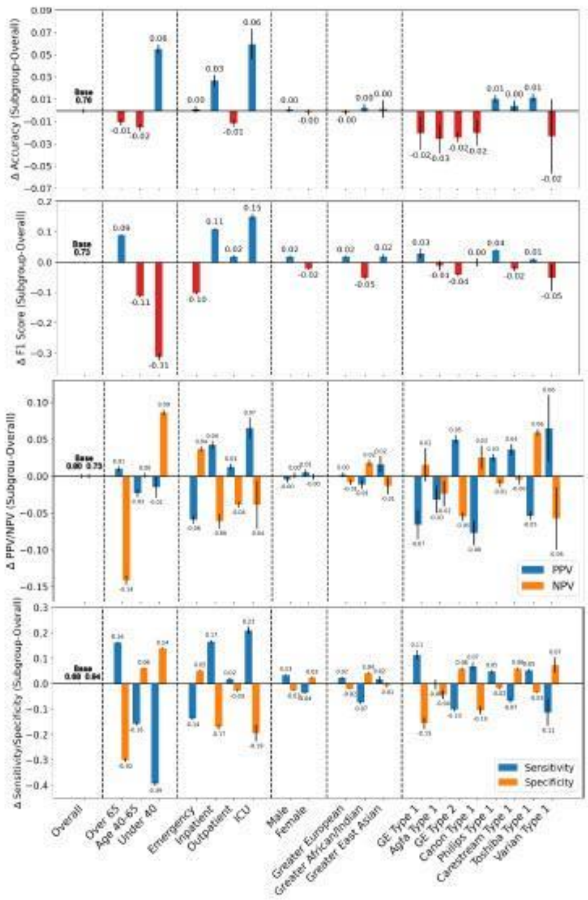

Fig.1 Example of suggested model card showing model performance analysis across social and non-social factors. In this case we analyzed a third-party classifier applied to 200,000 images from a tertiary care center[9]. We plot the difference in performance as measured by multiple metrics to demonstrate disparities.

Model Facts Card – Abnormality Classification of Screening Mammograms

Model Details

- A deep convolutional neural network enhanced by ResNet152V2 (He et al., 2016) pretrained on ImageNet (Deng et al., 2009), six additional dense layers were added
- Classifies screening mammogram patches as normal (BIRADS 1 or 2) or abnormal (BIRADS 0)

Intended Use:

- Screening mammograms classification for research purpose only

Factors:

- **Groups** include race (White, Black, other races), age, and 3 pathology classes (never biopsied, benign, and cancer)
- **Anatomic** tissue density
- **Image Findings** include mass, asymmetry, architectural distortion (AD), and calcification
- **Instrumental Factors** include 3 mammography device manufacturers
- **Environmental Factors** include screening mammography exam location

Metrics:

- Evaluation metrics include accuracy, area under the receiver operating characteristic curve (AUC), recall, precision, F1 score
- Bootstrap resampling ($n \in [1000, 13390]$) was used to generate 95% confidence interval (CI)

Training & Evaluation Data:

- 52,444 mammogram patches extracted from Emory Breast Imaging Dataset (EMBED) between 2013 to 2020 (Jeong et al., 2023)

Caveats & Recommendations:

- Does not represent performance at institutions outside Emory University
- Results may not be generalizable to other racial groups beside White and Black

Quantitative Analysis:

- Accuracy of 92.6% (95% CI = 92.0–93.2%), AUC of 0.975 (95% CI = 0.972-0.978) in binary patch classification of abnormality
- Patch classification performance was similar across race, age, and pathologic outcome; decreased performance was observed in dense breasts (density D), patches with architectural distortion (AD) compared to other imaging findings, and images taken by GE scanners

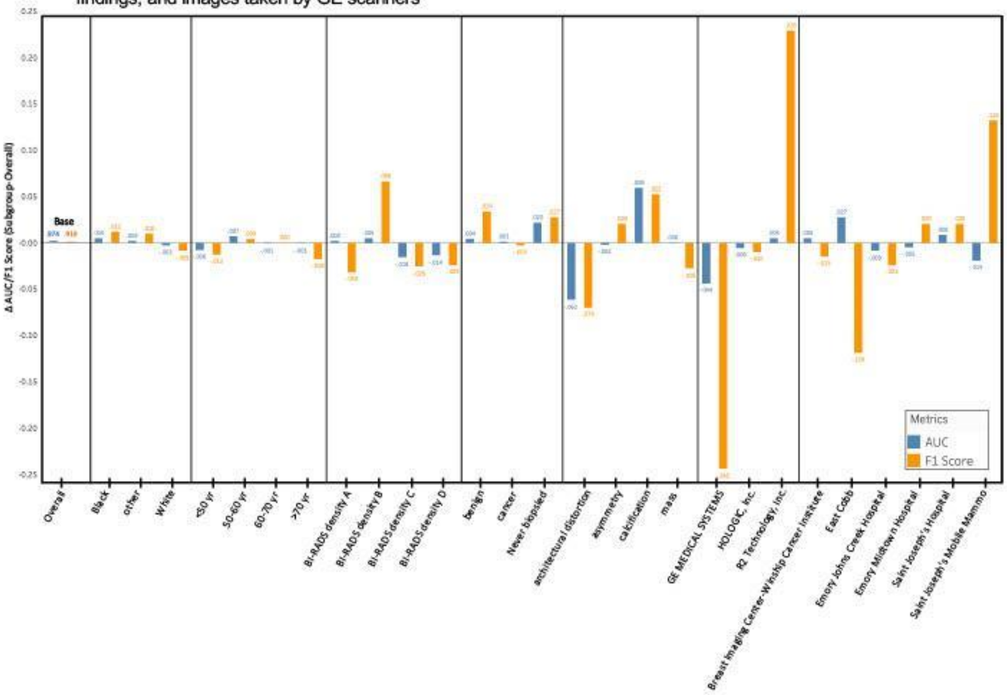

Fig 2. Model card for classification of abnormalities in screening mammography. Statistical analysis indicates that there are both social and non-social factors, such as anatomic factor (breast density), disease-dependent factors (architectural distortion), and instrumental factors, aggravating classification performance, which may lead to failure of the abnormality object detection in mammograms[10].

5. Conclusion

We propose a framework for considering and communicating a wider range of social and non-social factors in bias analysis, and push for its adoption in AI model fact cards. Analysis and communication of such a wider range of biases identify potential drivers of bias which pave the way to debiasing. Developers and end users may select or consider other factors based on their use case and available data. Additionally, they may re-consider gathering features that are not gathered regularly and we have shown they may impact the AI model performance. We are also aware that the fairness assessment is still performance-based, which means it is still relying on binary outcome and comparison to the ground truth label. This is not the best metrics, since the ground truth is biased. Therefore, having a good grade on such a model card does not guarantee that the algorithm is fair. In the end, the ultimate fairness metric is the impact on downstream clinical outcomes.

Author contributions:
All authors contributed to the creation of this commentary.

Funding Source Declaration:
LAC is funded by the National Institute of Health through NIBIB R01 EB017205.
We acknowledge the support of the Natural Sciences and Engineering Research Council of Canada (NSERC) Discovery Grant and Connected Mind Canada First Research Excellence Fund (CFREF) grant to L. S. K.
The funder played no role in study design, data collection, analysis and interpretation of data, or the writing of this manuscript.

Declaration of Interest:
All authors declare no financial or non-financial competing interests.

Data availability
The datasets used and/or analysed during the current study available from the corresponding author on reasonable request.

Code availability
The underlying code for this study and training/validation datasets are not publicly available but may be made available to qualified researchers on reasonable request from the corresponding author.

References:

1. Esteva, A. *et al.* Dermatologist-level classification of skin cancer with deep neural networks. *Nature* **542**, 115–118 (2017).

2. Haenssle, H. A. *et al.* Man against machine reloaded: performance of a market-approved convolutional neural network in classifying a broad spectrum of skin

lesions in comparison with 96 dermatologists working under less artificial conditions. *Ann. Oncol.* **31**, 137–143 (2020).

3. Seyyed-Kalantari, L., Zhang, H., McDermott, M. B., Chen, I. Y. & Ghassemi, M. Underdiagnosis bias of artificial intelligence algorithms applied to chest radiographs in under-served patient populations. *Nat. Med.* **27**, 2176–2182 (2021).
4. Gichoya, J. W. *et al.* AI recognition of patient race in medical imaging: a modelling study. *Lancet Digit. Health* **4**, e406–e414 (2022).
5. Sendak, M. P., Gao, M., Brajer, N. & Balu, S. Presenting machine learning model information to clinical end users with model facts labels. *NPJ Digit. Med.* **3**, 41 (2020).
6. Mitchell, M. *et al.* Model cards for model reporting. in *Proceedings of the conference on fairness, accountability, and transparency* 220–229 (2019).
7. Cirillo, D. *et al.* Sex and gender differences and biases in artificial intelligence for biomedicine and healthcare. *NPJ Digit. Med.* **3**, 81 (2020).
8. Obermeyer, Z., Powers, B., Vogeli, C. & Mullainathan, S. Dissecting racial bias in an algorithm used to manage the health of populations. *Science* **366**, 447–453 (2019).
9. Ahluwalia, M. *et al.* The Subgroup Imperative: Chest Radiograph Classifier Generalization Gaps in Patient, Setting, and Pathology Subgroups. *Radiol. Artif. Intell.* (2023).
10. Zhang, L. *et al.* Multivariate Analysis on Performance Gaps of Artificial Intelligence Models in Screening Mammography. *ArXiv Prepr. ArXiv230504422* (2023).

11. Seyyed-Kalantari, L., Liu, G., McDermott, M., Chen, I. Y. & Ghassemi, M. CheXclusion: Fairness gaps in deep chest X-ray classifiers. in *BIOCOMPUTING 2021: proceedings of the Pacific symposium* 232–243 (World Scientific, 2020).
12. Zhang, H. *et al.* Improving the fairness of chest x-ray classifiers. in *Conference on Health, Inference, and Learning* 204–233 (PMLR, 2022).
13. Pierson, E., Cutler, D. M., Leskovec, J., Mullainathan, S. & Obermeyer, Z. An algorithmic approach to reducing unexplained pain disparities in underserved populations. *Nat. Med.* **27**, 136–140 (2021).
14. Zhang, H., Lu, A. X., Abdalla, M., McDermott, M. & Ghassemi, M. Hurtful words: quantifying biases in clinical contextual word embeddings. in *proceedings of the ACM Conference on Health, Inference, and Learning* 110–120 (2020).
15. Ford, E. *et al.* Strategies for effective physics plan and chart review in radiation therapy: report of AAPM Task Group 275. *Med. Phys.* **47**, e236–e272 (2020).
16. Bohlender, S., Oksuz, I. & Mukhopadhyay, A. A survey on shape-constraint deep learning for medical image segmentation. *IEEE Rev. Biomed. Eng.* (2021).
17. Oakden-Rayner, L. *et al.* Validation and algorithmic audit of a deep learning system for the detection of proximal femoral fractures in patients in the emergency department: a diagnostic accuracy study. *Lancet Digit. Health* **4**, e351–e358 (2022).
18. McCormack, V. A. & dos Santos Silva, I. Breast density and parenchymal patterns as markers of breast cancer risk: a meta-analysis. *Cancer Epidemiol. Biomarkers Prev.* **15**, 1159–1169 (2006).
19. Checka, C. M., Chun, J. E., Schnabel, F. R., Lee, J. & Toth, H. The relationship of mammographic density and age: implications for breast cancer screening. *Am. J. Roentgenol.* **198**, W292–W295 (2012).

20. El-Bastawissi, A. Y., White, E., Mandelson, M. T. & Taplin, S. Variation in mammographic breast density by race. *Ann. Epidemiol.* **11**, 257–263 (2001).
21. Jeong, Y. J. *et al.* Current and emerging knowledge in COVID-19. *Radiology* **306**, e222462 (2023).
22. Burrill, J. *et al.* Tuberculosis: a radiologic review. *Radiographics* **27**, 1255–1273 (2007).
23. Salzer, H. J. *et al.* Clinical, diagnostic, and treatment disparities between HIV-infected and non-HIV-infected immunocompromised patients with Pneumocystis jirovecii pneumonia. *Respiration* **96**, 52–65 (2018).
24. Kim, J. H. *et al.* Visually isoattenuating pancreatic adenocarcinoma at dynamic-enhanced CT: frequency, clinical and pathologic characteristics, and diagnosis at imaging examinations. *Radiology* **257**, 87–96 (2010).
25. Irvin, J. *et al.* Chexpert: A large chest radiograph dataset with uncertainty labels and expert comparison. in *Proceedings of the AAAI conference on artificial intelligence* vol. 33 590–597 (2019).